

The electrical conductivity of hydrogenated nanocrystalline silicon investigated at the nanoscale

This article has been downloaded from IOPscience. Please scroll down to see the full text article.

2010 Nanotechnology 21 045702

(<http://iopscience.iop.org/0957-4484/21/4/045702>)

View [the table of contents for this issue](#), or go to the [journal homepage](#) for more

Download details:

IP Address: 130.209.6.40

The article was downloaded on 25/04/2012 at 17:02

Please note that [terms and conditions apply](#).

The electrical conductivity of hydrogenated nanocrystalline silicon investigated at the nanoscale

Daniela Cavalcoli¹, Francesca Detto², Marco Rossi³,
Andrea Tomasi⁴ and Anna Cavallini

Physics Department, University of Bologna, viale C Berti Pichat 6/ I-40127, Bologna, Italy

E-mail: cavalcoli@bo.infn.it

Received 27 October 2009, in final form 16 November 2009

Published 10 December 2009

Online at stacks.iop.org/Nano/21/045702

Abstract

Hydrogenated nanocrystalline silicon (nc-Si:H) is a multiphase, heterogeneous material, composed of Si nanocrystals embedded in an amorphous matrix. It has been intensively studied in the last few years due to its great promise for photovoltaic and optoelectronics applications. The present paper aims to study the current transport mechanisms in nc-Si:H by mapping the local conductivity at the nanoscale. The role of B doping in nc-Si:H is also investigated. Conductivity maps are obtained by atomic force microscopy using a conductive tip. Differences and similarities between intrinsic and doped nc-Si:H conductivity maps were observed and these are also explained on the basis of recently published computational studies.

(Some figures in this article are in colour only in the electronic version)

1. Introduction

Hydrogenated nanocrystalline silicon (nc-Si:H) has attracted great interest in the last few years due its great promise for photovoltaic and optoelectronic applications. Since the discovery of the higher stability against light exposure of solar cells based on nc-Si:H with respect to that of ones based on a-Si:H, this material has been intensively studied for both applications and basic physics.

nc-Si:H can be easily grown at substrate temperatures ranging from 100 to 300°C by plasma enhanced chemical vapour deposition (PECVD) methods. The composition of the films can be controlled by varying the hydrogen dilution ratio during deposition, yielding materials that span the transition from the amorphous to the microcrystalline state, with increasingly larger grain size and crystalline fraction at lower dilution ratios.

¹ Author to whom any correspondence should be addressed.

² Present address: IMEM-CNR Istituto dei Materiali per l'Elettronica ed il Magnetismo Parco Area delle Scienze, 37/A—43100 Parma, Italy.

³ Present address: ESTELUX s.r.l., Via G. Marconi 29, San Pietro in Gu Padova, Italy.

⁴ Present address: X Group SPA Via dell' Artigianato, Z.I. Vanzo di S Pietro Viminario, Padova, Italy.

In spite of the wide interest in the applications of this material as the intrinsic layer in 'micromorph' solar cells [1] and the consequent interest in its electronic transport properties [2], the understanding of these properties is still at a pioneering level. The structure of thin film nanocrystalline silicon can be described qualitatively as a collection of silicon crystallites from nanometre to micron scale embedded in a hydrogenated amorphous silicon (a-Si:H) matrix. During the growth the crystallites coalesce, forming columnar-like clusters in the direction of the film growth [2]. The complexity of nc-Si:H is, therefore, due to the coexistence of different phases: crystalline nanograins, nanocrystalline columns, hydrogenated amorphous Si (a-Si:H), defects (i.e. boundaries between the different phases) and voids. In addition there can be several kinds of disordered silicon tissues between the different phases [3]. All these phases may be involved in the transport mechanism, and charge transfer between them may involve tunnelling and thermionic emission, or a connected network of aggregates of such components.

Numerous papers have been published on measurements of macroscopic transport in nc-Si:H and essentially all possible current flow scenarios following from the above described heterogeneous structure have been proposed [2, 4]. The

electrical conduction in composite systems is determined by two mechanisms: percolation in a continuous conducting network and/or tunnelling between isolated conducting particles, grains, crystallites, etc. In pioneering works on such systems, these two mechanisms have been considered separately. For nc-Si:H the charge transport models that have been proposed are based on hopping and barrier-limited transport, or a combination of the two. These models do not account for the saturation in Arrhenius plots of the conductivity observed at low temperatures. A heterogeneous model for microcrystalline silicon based on the framework of a fluctuation-induced tunnelling mechanism was recently proposed [4].

Macroscopic measurements can clarify which transport mechanism is dominant, but not the specific network responsible for the conduction. In other words macroscopic transport measurements can indicate *how* but not *where* (i.e. in which phase of the film) the conduction takes place. For when the crystalline phase is larger in volume than the amorphous one, two scenarios have been considered in microscopic analyses: transport via the crystallite columns and transport in the disordered tissue that encapsulates them.

The choice between these two alternatives is not simple due to conflicting data: on one hand, Rezek *et al* [5], by means of microscopic analyses, showed that electronic transport occurs through the columns (i.e. through the crystallites that constitute them), while, on the other hand, the microscopic and macroscopic data of Azulay *et al* and Balberg *et al* [3, 6] indicated that transport occurs in the disordered tissue surrounding columns or crystallites. The discrepancy between the microscopic results of these two groups has been explained [3] by taking into account the different procedures of growth of the Si films: the samples investigated by Azulay *et al* [3] were grown under high vacuum, while those studied by Rezek *et al* [5] could have contained considerable O concentrations that could yield unintentional doping of the layers.

Hence, the localization of the current flow in nc-Si:H still needs to be clarified.

Moreover, B doping significantly enhances the complexity of the system; in fact, transport mechanisms and the impurity incorporation are still under investigation. Early studies on porous Si [7] have shown that the ionization of impurities in low dimension systems is strongly quenched with respect to that for the bulk. The incorporations of group III (B and Al), group IV (C and Ge), and group V (N and P) impurities in Si nanocrystallites were investigated by means of an *ab initio* pseudopotential method [8, 9]. The authors find that the acceptor (group III) and donor (group V) levels become deep as the nanocrystallites become small. The mechanisms of transport in lightly boron-doped microcrystalline Si were investigated by means of dark conductivity measurements; a 'diffusional model' considering the Einstein relation, conductivity, the diffusion coefficient, and the hopping probability was proposed [10].

Thus a full understanding of the ionization processes and transport mechanisms for doped low dimensional systems is still far from being reached.

In order to address these important issues a detailed and systematic study of the local conductivity in intrinsic and B-doped hydrogenated nanocrystalline Si is presented here. By probing the local conductivity, the following questions can be answered: Where does the current flow in nc-Si:H? Can B doping significantly enhance the conductivity of nc-Si:H films?

2. Experimental details

Several nc-Si:H films, grown on different substrates (silicon, oxidized silicon, Corning glass, ITO and ZnO on Corning glass) by LEPECVD (low energy plasma enhanced chemical vapour deposition) were examined. Further details on the deposition conditions and structural properties of the films can be found in [11, 12]. Among the CVD variant growth methods used for producing nc-Si:H (such as hot wire CVD and the standard plasma enhanced CVD), LEPECVD is of major interest due to the low ion energy, which causes only limited surface damage.

Intrinsic (nominally undoped) nc-Si:H films, approximately 1 μm thick, were deposited at dilution factors d ($d = \Phi(\text{SiH}_4)/(\Phi(\text{SiH}_4) + \Phi(\text{H}_2))$, with Φ the gas flux) ranging from 1% to 60% with a substrate temperature ranging from 210 to 280 °C. Moreover, B-doped nc-Si films 50–90 nm thick were grown by LEPECVD on Corning glass or on ZnO coated Corning glass with $d = 1\%$ and varying doping densities, which were obtained by varying the $\text{B}_2\text{H}_6/\text{SiH}_4$ ratio.

AFM analyses were carried out using a Solver P47H-Pro instrument manufactured by NT-MDT. Conductive atomic force microscopy (C-AFM) allows for local electrical conductivity analyses at the nanoscale. A constant positive bias was applied to the probe while the AFM operated in constant force mode (contact mode). Conductive tips purchased from a few manufacturers (Nanosensors, NT-MDT) with different conductive coatings (Pt, Pt/Ir, W_2C , doped diamond) were used. The samples were grounded through the bottom or upper, or both, electrical contacts made with gallium–aluminium. The bottom contact was made beneath the substrate and the upper contact on the thin film surface. C-AFM maps obtained with both contacts or with just one of them did not show any significant differences. All the C-AFM maps were obtained in air at small load conditions (normal force lower than 600 nN), and special care was taken during the measurements in order to avoid significant artefact effects [13].

3. Results

An extensive analysis for several sample sets, grown at various temperatures (from 210 to 280 °C), growth rates (from 0.1 to 4 nm s^{-1}), and dilution rates (from 1 to 60%), and on various substrates (Si, glass, transparent conductive oxides on glass), has been carried out. Growth parameters were found to influence several sample characteristics, such as the crystal fraction as measured by Raman spectroscopy, optical properties (absorption coefficient), and the macroscopic conductivity [11, 12]. In contrast the C-AFM maps turned out to be almost independent of the kind of substrate and the growth temperature. The main parameter affecting the

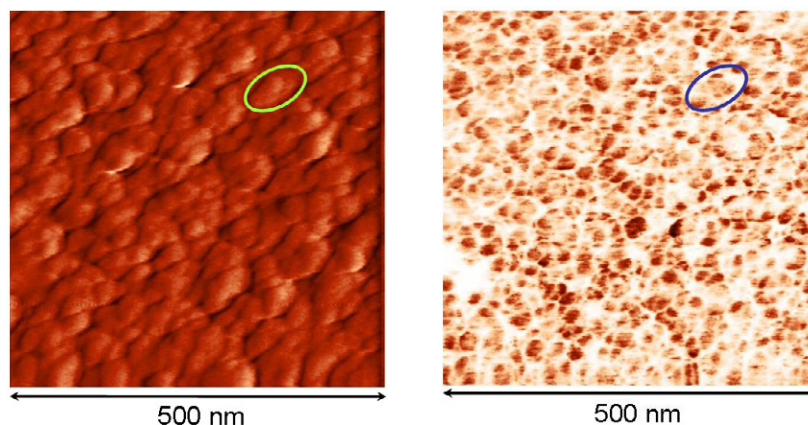


Figure 1. AFM topographical (left) and C-AFM current (right) maps obtained for intrinsic nc-Si grown on Si, with $d = 50\%$, $T = 280^\circ\text{C}$, growth rate $= 3.6 \text{ nm s}^{-1}$. The applied bias potential is 3 V; the greyscale ranges from 0 to 25 nm (left) and from 0 (white) to 1.8 (dark) nA (right). The circles indicate what in the text is called a ‘domain’.

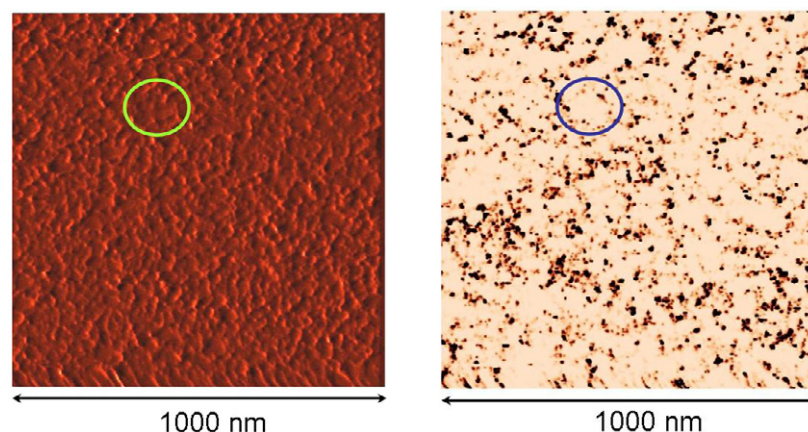


Figure 2. AFM maps of B-doped nc-Si:H grown on Corning glass. Silane dilution 1%, diborane dilution $\text{DR} = \text{B}_2\text{H}_6/\text{SiH}_4 = 3.6\%$, growth temperature $T = 250^\circ\text{C}$, bias potential 0.5 V; the greyscale ranges from 0 to 37 nm (left), from 0 (white) to 10 (dark) nA (right). The circles indicate the domains.

current maps is the crystal fraction: intrinsic samples with very low crystal fraction (below 20%) showed current values under the detection limit of the system (some tens of pA). As the systematic study that we carried out on many samples grown with different growth parameters did not show any further dependence of the C-AFM maps on the growth parameters, some typical results obtained for the intrinsic and B-doped nc-Si:H will be presented here, together. The growth parameters will be specified for each map presented.

Figure 1 shows one example of topography (left) and current-AFM (right) maps of undoped nc-Si:H film grown on Si, obtained with a bias voltage of 3 V. The current map, at constant applied bias, represents a dark conductivity map. The topography map shows the presence of large (50–100 nm diameter) ‘domains’; one of these domains is indicated by a circle in figure 1. The domains probably represent clustering of several nanocrystals, whose diameter, as measured by transmission electron microscopy for the same samples (TEM) [14, 15], varies between 5 to 15 nm. Within these domains the C-AFM map (figure 1, right) shows a number of conductive grains separated from each other by non-conductive tissue. It is worth noting that the conductive

grains are mainly located within the domains. The conductance values of the Si nanocrystallites (NCs) range from 0.2 to 0.3 nS.

This behaviour is typical for all the intrinsic layers examined using C-AFM, irrespective of their substrate, deposition temperature and growth rate. In more detail, similar C-AFM maps were obtained for all the intrinsic samples with a crystallinity fraction larger than 30%, as measured from Raman spectra [11], while samples with lower crystallinity values showed mostly non-conducting characteristics, sometimes with current values lower than the detection limit of the system.

Figure 2 shows typical topography (left) and current-AFM (right) maps of a B-doped nc-Si film grown on glass. The C-AFM map was obtained by applying a bias voltage of 0.5 V. The different behaviours as regards the intrinsic samples appear clearly from the maps: conductive nanocrystallites surrounded by non-conductive tissue are evident in the C-AFM map, but the conductive grains are mainly located at the domain boundaries. Moreover, the Si NC conductance values differ strongly: while in intrinsic layers the Si NCs show conductance values around 0.2 nS, in doped layers

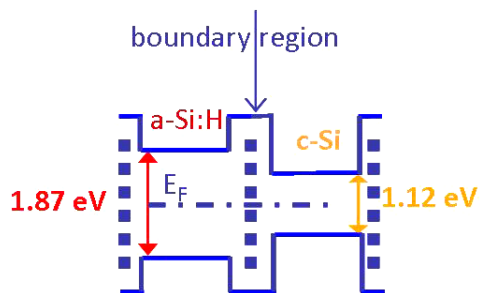


Figure 3. Schematic band diagram of nc-Si:H.

the conductance values are spread over a large range, from 2 to 8 nS. Similar results have been obtained for all the films examined, independently of their growth temperature and substrate.

The results of C-AFM analyses of intrinsic and B-doped nc-Si:H films can be summarized as follows. In all the films examined (both doped and undoped) the charge conduction occurs via the Si nanocrystals (NCs) in good agreement with literature data [5]. In contrast, the discrepancy between the present result and the ones reported in [3] is evident. This discrepancy has been attributed by the authors of [3] to the unintentional doping with O that could have occurred with the samples investigated in [5]. Furthermore, this discrepancy could also be explained by the fact that the application of large bias voltages (of the order of 10 V) in AFM can generate a persistent, spatially localized modification of electronic properties of undoped amorphous and microcrystalline silicon films [5] or a strong mechanical erosion of the conductive tips [13]. Both these effects could contribute to the explanation of the differences between maps obtained by different groups working with samples grown differently and in different bias and ambient conditions.

This result can be explained on the following basis. nc-Si:H is made up of several contributions: Si NCs, amorphous phase, boundaries between different phases, impurities (mainly O and H), voids, extended defects. We can reasonably imagine that the Si NCs are separated from each other by defects and phase boundaries which behave as preferential sites for impurity segregation, thus creating a potential barrier to carrier conduction. Moreover, the amorphous phase has a band gap of 1.87 eV, as evaluated by surface photovoltage spectroscopy [16], significantly larger than the band gap of the Si nanocrystals. Following this picture, sketched in figure 3, it can be concluded that Si NCs could represent the sites where free carriers are strongly localized, and thus appear more conductive with respect to the surrounding tissue.

Figure 4 shows the frequency distribution of the maximum current values (which roughly correspond to the current values of the Si NCs) for a typical map of undoped and doped nc-Si:H films. In order to allow comparisons, the current values have been divided by the applied voltage in each case. By comparing the C-AFM maps (figures 1 and 2) and the frequency distributions (figure 4), it can be noted that the average conductance value of B-doped nc-Si:H is more than one order of magnitude larger than that of undoped nc-Si:H. In

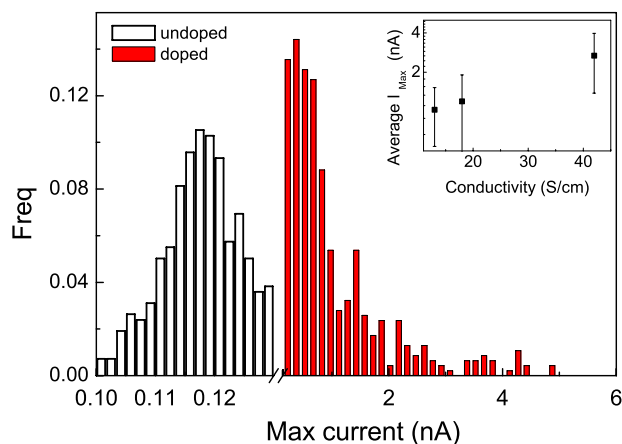


Figure 4. Frequency distribution of the maximum current values (corresponding to the Si NC current) measured for undoped (white) and doped (red) nc-Si:H samples. For the sake of comparison the current values have been normalized with respect to the bias voltage (3 V for the intrinsic layer, 0.5 V for the doped layers). In the inset, average maximum current values obtained for doped films have been plotted versus the measured macroscopic conductivity [17].

the inset of figure 4 the maximum current values averaged over the map are plotted as a function of the measured macroscopic conductivity for films doped with B₂H₆/SiH₄ in ratios ranging from 5 to 20% [17]. The current values scale well with the conductivity (which in turn scales well with the B dilution ratio [17]). This means that B doping actually changes the conductivity of nc-Si:H films.

From the comparison between the C-AFM maps reported in figures 1 and 2, it can be noted that in intrinsic layers the conductive NCs are located mainly within the domains evident in the AFM maps, while in doped layers the conductive NCs are mainly located within the boundaries between the domains.

The distribution of the NC current values also changes between intrinsic and doped layers (figure 4). While the frequency distribution of the current values in intrinsic films is a nearly symmetrical one-peak Gaussian-like distribution, the one for doped layers is strongly non-symmetrical and shows some other minor peaks. Moreover, for doped films a wide range of conductance values can be evidenced: the NC conductance values can double or even quadruple within the same map. The NC frequency distribution (figure 4) shows that a significant amount of Si NCs have current values lower than the map average, while a very small amount of Si NCs have current values larger than the map average.

4. Discussion and conclusions

In order to explain these features the following hypothesis can be advanced. By TEM analyses on the same samples, the diameters of the Si NCs have been determined to vary between 5 and 15 nm [14, 15]. In some cases the Si NCs conglomerate, forming columns, and in other cases they remain isolated in the amorphous matrix. The non-uniform strain distribution during film growth could lead to a strong inhomogeneity of the NC size distribution in the film. Isolated NCs could more easily cluster when located within a domain border than when located

within the domains. In intrinsic layers, isolated NCs located in the domains are conductive due to the spatial localization of carriers, as explained before, which can be more effective for single NCs, while large NC clusters located at the domain borders can be less conductive.

Conversely, in doped layers, clusters of Si NCs located at the domain boundaries can be more conductive due to the larger doping efficiency of B in large NCs. In fact, computational and experimental studies demonstrated the size dependence of the formation energy of B in Si NCs [8, 9] and the suppression of PL in annealed B-doped Si NCs [18]. The computational study [8] showed a linear increase of the formation energy versus the inverse cluster radius. Both the studies reached the conclusion that large Si NCs can easily sustain the doping. Moreover, a further theoretical study showed that group III impurities introduce in Si NCs shallow acceptor levels in the gap that become shallower as the size of the Si NCs increases [9]. Therefore, it can be concluded that small, isolated Si NCs are conductive in intrinsic layers due to quantum confinement effects, while large, clustered Si NCs are conductive in B-doped layers due to the size effect of B doping efficiency.

The frequency distribution of current values can be seen as a direct consequence of this size effect: in intrinsic layers the distribution of current values follows the size distribution of Si nanostructures, which are randomly distributed around an average value.

In contrast, in doped layers, the asymmetrical distribution and the wide range of conductance values can be explained by assuming that not all the Si NCs are efficiently doped—in fact that only the ones with dimensions larger than some threshold value are efficiently doped.

To summarize, C-AFM analyses of hydrogenated nanocrystalline Si have shown that the electrical conduction occurs via the Si crystallites, in intrinsic as well as in doped layers. Moreover, B doping significantly enhances the conductivity of the nc-Si:H films, but the doping efficiency is strongly dependent on the microstructure of the film.

Acknowledgments

This work was entirely funded by the European Commission, Nanophoto project Contract no. 013944 (www.nanophoto.unimib.it). G Isella and D Charastina of L-NESS Lab, in

Como, Italy, are gratefully acknowledged for carrying out the sample growth.

References

- [1] Shah A V, Meier J, Vallat-Sauvain E, Wyrsh N, Kroll U, Droz C and Graf U 2003 *Sol. Energy Mater. Sol. Cells* **78** 469
- [2] Fejfar A, Beck N, Stuchlikova H, Wyrsh N, Torres P, Meier J, Shah A and Kocka J 1998 *J. Non-Cryst. Solids* **227–230** 1006
- [3] Azulay D, Balberg I, Chu V, Conde J P and Millo O 2005 *Phys. Rev. B* **71** 113304
- [4] Konezny S J, Bussac M N and Zuppiroli L 2008 *Appl. Phys. Lett.* **92** 012107
- [5] Rezek B, Stuchlýk J, Fejfar A and Kocka J 2002 *Appl. Phys. Lett.* **92** 587
- [6] Balberg I, Dover R, Naides J, Conde P and Chu V 2004 *Phys. Rev. B* **69** 035203
- [7] Polisski G, Heckler H, Kovalev D, Schwartzkopff M and Koch F 1998 *Appl. Phys. Lett.* **73** 1107
- [8] Cantele G, Degoli E, Luppi E, Magri R, Ninno D, Iadonisi G and Ossicini S 2005 *Phys. Rev. B* **72** 113303
- [9] Ramos L E, Degoli E, Cantele G, Ossicini S, Ninno D, Furthmüller J and Bechstedt F 2007 *J. Phys.: Condens. Matter* **19** 466211
- [10] Dussan A and Buitrago R H 2005 *J. Appl. Phys.* **97** 043711
- [11] Le Donne A, Binetti S, Isella G, Pichaud B, Texier M, Acciarri M and Pizzini S 2008 *Appl. Surf. Sci.* **254** 2804
- [12] Binetti S, Acciarri M, Bollani M, Fumagalli L, von Känel H and Pizzini S 2005 *Thin Solid Films* **487** 1925
- [13] Cavalcoli D, Rossi M, Tomasi A and Cavallini A 2009 *Nanotechnology* **20** 045702–8
- [14] Cavallini A, Cavalcoli D, Rossi M, Tomasi A, Pichaud B, Texier M, Le Donne A, Pizzini S, Chrastina D and Isella G 2008 *Proc. 15th Conf. on Microscopy of Semiconducting Materials (Cambridge) (Springer Proceedings in Physics vol 120)* ed A G Cullis and P A Midgley (Bristol: Canopus Publishing) pp 301–4
- [15] Texier M et al 2008 *Proc. 15th Conf. on Microscopy of Semiconducting Materials (Cambridge) (Springer Proceedings in Physics vol 120)* ed A G Cullis and P A Midgley (Bristol: Canopus Publishing) pp 305–8
- [16] Cavallini A, Cavalcoli D, Rossi M, Tomasi A, Pizzini S, Chrastina D and Isella G 2007 *Physica B* **401/402** 519
- [17] Micard G et al 2009 *Proc. 23rd Int. Conf. on Amorphous and Nanocrystalline Semiconductors; Phys. Status Solidi c* at press
- [18] Fujii M, Yamaguchi Y, Takase Y, Ninomiya K and Hayashi S 2004 *Appl. Phys. Lett.* **85** 1158